Preprints of the 21st IFAC World Congress (Virtual)
Berlin, Germany, July 12-17, 2020

Dynamic Analysis and Control of the Hepatitis C Virus

Mauricio Castaño-Arcila, Alberto Ramírez-Hurtado, Carlos Galvéz de León, Jesús Rodríguez-González

Center for Research and Advanced Studies of the National Polytechnic Institute, Unit Monterrey, Apodaca 66600 México, (e-mail: mcastanoa@cinvestav.mx, alberto.ramirez@cinvestav.mx,carlos.galvez@cinvestav.mx, jrodriguez@cinvestav.mx)

Abstract: The Hepatitis C Virus is the main cause of chronic liver diseases. The acute stage of infection is usually asymptomatic, and persistence in most of the infected individuals leads to chronic hepatitis, hepatic cirrhosis, and, finally, hepatocellular carcinoma. In order to avoid the chronic or advanced stages of this disease, when HCV is detected, cells activate the immune response mediated by interferon. Interferon is released by the infected hepatocytes and surrounding sentinel cells. Interferon activates the JAK-STAT signaling pathway and stimulates several ISG genes. Recently, it has been reported that only seven of them show a significant anti-HCV response. The aim of this study was to investigate, from a mathematical-modeling point of view, whether ISG over-expression leads the system to an irreversible clearance state. A mathematical model for the molecular machinery involved in cells infected with hepatitis C and the immune response was used to reproduce viral dynamics. The model considers seven ISG proteins. Our results suggest that the ISG proteins play an essential role in the hepatitis dynamics, and there is a possibility of produce the clearance state. Their robustness is evaluated.

Keywords: Systems biology, dynamics and control, cellular systems, control of physiological variables, physiological model, modeling and identification of nonlinear systems.

1. INTRODUCTION

Hepatitis is an inflammation of the liver and has a broad spectrum of presentations from a lack of symptoms to severe liver failure. A viral infection most commonly causes it. Hepatitis C virus (HCV) infection is a major cause of chronic liver disease. The innate immune response is the first line of defense of the human body against HCV infection immediately after infection. Production of interferon (IFN) is one of the primary host defense mechanisms and plays a critical role in the human immune response. IFN leads to the activation and regulation of the cellular components of innate immunity. The virus replicates continuously in hepatocytes, which constitute 80% of the liver mass. A characteristic of HCV infection is the extraordinary ability of the virus to persist in a majority of infected people.

The interplay between the intracellular IFN signaling network and HCV is schematically represented in Fig. 1. HCV replication occurs in the cytoplasm; a positive-strand of RNA is used to produce a negative-strand that is used as a template for RNA production. Interferon activates the JAK-STAT signaling pathway, which induces the transcription of several IFN-stimulated genes (ISG). The translation of ISG mRNAs produces ISG proteins. These ISG proteins inhibit HCV replication. At the same time, the virus blocks the JAK-STAT signaling network inhibiting ISG transcription.

Nowadays, it is known that there are more than 300 ISG genes regulated by IFN through the JAK-STAT signaling pathway. However, it has been reported that only seven ISG proteins contribute to the suppression of HCV replication by IFN, Metz et al. (2013).

Padmanabhan and colleagues studied HCV infection of patients treated with high doses of IFN and ribavirin. Using mathematical modeling, they predict that treatment failure has a consequence of the bistability of the IFN signaling network, Padmanabhan et al. (2014).

Gene therapy is the transfer of genetic material to a patient to treat a disease. During the last twenty years, mRNA-vaccines based technologies have been investigated extensively for infectious disease prevention, Schlake et al. (2019).

Motivated by the above considerations and taking into account a number of experimental and theoretical studies have allowed the exploration of HCV dynamics, In this work, we address the following question to understand, which is the interplay between hepatitis C virus and immune response: how can the interaction between HCV and immune response be modulated in infected cells? We investigated whether the transitions between the two branches of stable, steady states become irreversible when ISG proteins are overexpressed, Guidi and Goldbeter (1997). We built a minimal mathematical model based on the model reported by Padmanabhan, where the seven ISG proteins

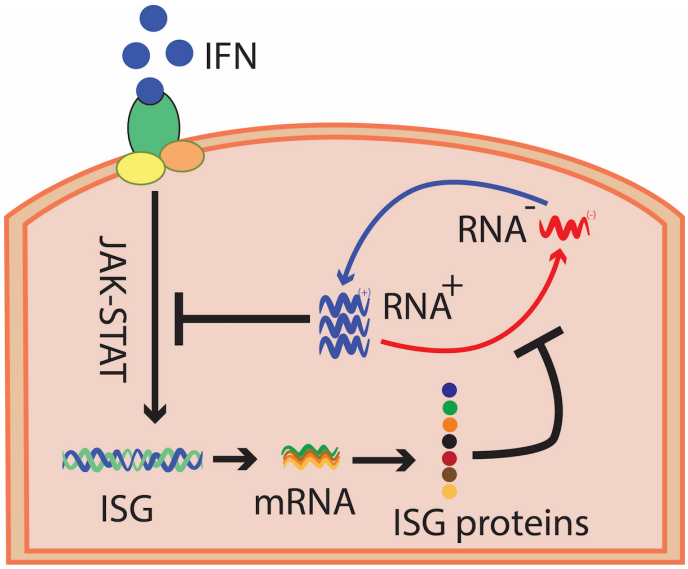

Fig. 1. Graphical representation of the molecular machinery involved in hepatocyte cell infected with HCV and the innate immune response. Simplified representation of the double negative feedback when seven ISG proteins inhibit HCV. HCV inhibits transduction of ISG genes.

interactions with the HCV in infected cells were explored. Clearance state is the physiological state objective.

2. MATHEMATICAL MODEL

To gain insight into the double feedback loop present in the IFN signaling network in the presence of HCV, we developed a minimal mathematical model, which contains two feedback loops while still capturing the qualitative behavior of the extended model from Padmanabhan et al. (2014). The mathematical model is formed by sixteen differential equations to describe the molecular dynamics depicted in Fig. 1.

The following Eqs. 1 and 2 represents the concentration of positive (V_P) and negative (V_N) strands HCV RNA, inside a cell as a function of time. Parameters k_1 and k_2 are the maximal production rate of positive and negative strand HCV RNAs. Second factor in positive term of Eq. 1 represents HCV inhibition effect of six ISG proteins inside a cell. Parameters K_{r_n} stand for the half-inhibition constant. Third factor is the carrying capacity of the cell for HCV. Parameter K_c correspond to carrying capacity of the cell. HCV RNA is degraded by RNaseL protein. Parameters K_{d_7} is the half-inhibition constant, and P_7 represents the RNaseL protein concentration.

$$\frac{d[V_P]}{dt} = k_1\left(\prod_n \frac{K_{r_n}}{K_{r_n}+[P_n]}\right)\left(1-\frac{[V_P]+[V_N]}{Kc}\right)[V_N] - \frac{\mu_1}{\frac{K_{d_7}}{K_{d_7}+[P_7]}}[V_P] \quad (1)$$

$$\frac{d[V_N]}{dt} = k_2\left(\prod_n \frac{K_{r_n}}{K_{r_n}+[P_n]}\right)\left(1-\frac{[V_P]+[V_N]}{Kc}\right)[V_P] - \mu_2[V_N] \quad (2)$$

Where $n \in \{IFIT3, IFITM1, IFITM3, TRIM14, Viperin, PLSCR1\}$.

Dynamics of each one ISG mRNAs and ISG proteins are given by the differential equations 3 and 4.

$$\frac{d[M_i]}{dt} = k_{m_i}\frac{[IFN]}{K_{i_{IFN}}+[IFN]}\frac{K_H}{K_H+[V_P]} - \mu_{m_i}[M_i] \quad (3)$$

$$\frac{d[P_i]}{dt} = k_{p_i}[M_i] - \mu_{p_i}[P_i] \quad (4)$$

Where $i \in \{IFIT3, IFITM1, IFITM3, TRIM14, Viperin, PLSCR1, RNaseL\}$.

The meaning of parameters is as follows. Parameters k_{m_i} represent the IFIT3, IFITM1, IFITM3, TRIM14, Viperin, PLSCR1, and RNaseL transcription rates, respectively. Parameters k_{p_i} denote the IFIT3, IFITM1, IFITM3, TRIM14, Viperin, PLSCR1, and RNaseL translation rates, respectively. Parameters μ_{m_i} and μ_{p_i} stand for the IFIT3, IFITM1, IFITM3, TRIM14, Viperin, PLSCR1, and RNaseL mRNA and protein degradation rates, respectively. Second factor in positive term of Eq. 3 represents IFN effect in presence of HCV. Parameters $K_{i_{IFN}}$ stand for the IFN dose at which the IFIT3, IFITM1, IFITM3, TRIM14, Viperin, PLSCR1, and RNaseL transcription rates are half-maximal, respectively. Third factor stands for HCV effect in JACK-STAT response. Parameter K_H represents the half-inhibition constant of the ISG production associated with HCV.

2.1 Parameter values

All parameter values used in Eqs. (1)-(4) have biological relevance and were estimated from published experimental data. mRNA transcription rates were estimated using the ISG mRNA sequence lengths from the NCBI database and the rate of stable RNA synthesis (306000 nucleotides per hour), Dennis and Bremer (2008). Protein translation rates were obtained using the ISG protein length from the NCBI database and the global translation rate (39600 amino-acid per hour) reported by Siwiak and Zielenkiewicz (2013). The resulting parameter values are tabulated in Table 1.

3. RESULTS

To validate the feasibility of the deterministic model, a set of experiments by Garaigorta & Chisari was simulated Garaigorta and Chisari (2009). Multiplicity of infection (MOI) is defined as the ratio of the number of virus particles to the number of target cells present in a defined space. In these experiments, the immortalized human hepatocytes were infected with the HCV JFH-1 genotype, and the viral load was measured at different post-infection times. They experimentally follow the hepatitis virus infection dynamics in a cell line at a given multiplicity of infection ($MOI = 3$). In these experiments,

cells were no treated with interferon, IFN=0. They report the time course of the level of double-stranded RNA. We mimicked these experiments by numerically solving the model equations with the following set of initial conditions: $(V_p(0) = 3,\ V_n(0) = 0, M_i(0) = 0,\ P_i(0) = 0,\ i \in \{IFIT3, IFITM1, IFITM3, TRIM14, Viperin, PLSCR1, RNaseL\}$, molecules/cell, respectively. We set $IFN = 0$. The model equations were then numerically solved for 70 h to guarantee the system reach the steady-state. We can see in Fig. 2, the dynamics of the levels of positive-stranded RNA. The simulation results have been compared with the experimental data (green circles). The virus replicates until it reaches its maximal viral load the system behavior under those condition match with the experimental results. Furthermore, our simulation results are in agreement with experimental results and with previous modeling works, Padmanabhan et al. (2014). We found a linear correlation between experimental and *in-silico* results, with $R^2 = 0.97$.

We further analyzed the stability of the intracellular IFN signaling network and HCV. To calculate the steady states of the model, we followed the graphical method proposed by Ferrell et al., Ferrell and Xiong (2001). We consid-

Table 1. Parameter values

Parameter	Value (units)	Source
k_1	9.46×10^{-1} (h^{-1})	Padmanabhan et al. (2014)
k_2	4.73×10^{-2} (h^{-1})	Padmanabhan et al. (2014)
Kc	317.54 (mol cell)$^{-1}$	Padmanabhan et al. (2014)
μ_1	4.62×10^{-2} (h^{-1})	Ribeiro et al. (2012)
μ_2	5.77×10^{-2} (h^{-1})	Ribeiro et al. (2012)
k_{m1}	124 mol (cell h)$^{-1}$	NCBI NM_001031683.3
k_{m2}	417 mol (cell h)$^{-1}$	NCBI NM_003641.3
k_{m3}	451 mol (cell h)$^{-1}$	NCBI NM_021034.2
k_{m4}	171 mol (cell h)$^{-1}$	NCBI NM_033220.1
k_{m5}	107 mol (cell h)$^{-1}$	NCBI AF442151.1
k_{m6}	137 mol (cell h)$^{-1}$	NCBI NM_021105.2
k_{m7}	72 mol (cell h)$^{-1}$	NCBI NM_021133.3
$K1_{IFN}$	7 IU ml^{-1}	Padmanabhan et al. (2014)
$K2_{IFN}$	45 IU ml^{-1}	Padmanabhan et al. (2014)
$K3_{IFN}$	109 IU ml^{-1}	Padmanabhan et al. (2014)
$K4_{IFN}$	21 IU ml^{-1}	Padmanabhan et al. (2014)
$K5_{IFN}$	140 IU ml^{-1}	Padmanabhan et al. (2014)
$K6_{IFN}$	14 IU ml^{-1}	Padmanabhan et al. (2014)
$K7_{IFN}$	21 IU ml^{-1}	Padmanabhan et al. (2014)
μ_{P1}	2.9×10^{-2} (h^{-1})	Sharova et al. (2009)
μ_{P2}	6.19×10^{-2} (h^{-1})	Sharova et al. (2009)
μ_{P3}	$6.19 \times 10^{-2} (h^{-1})$	Sharova et al. (2009)
μ_{P4}	3.75×10^{-2} (h^{-1})	Sharova et al. (2009)
μ_{P5}	$6.08 \times 10^{-2} (h^{-1})$	Sharova et al. (2009)
μ_{P6}	$6.08 \times 10^{-2} (h^{-1})$	Sharova et al. (2009)
μ_{P7}	2.39×10^{-2} (h^{-1})	Sharova et al. (2009)
μ_{m1}	9.27×10^{-2} (h^{-1})	Sharova et al. (2009)
μ_{m2}	6.21×10^{-2} (h^{-1})	Sharova et al. (2009)
μ_{m3}	7.47×10^{-2} (h^{-1})	Sharova et al. (2009)
μ_{m4}	1.59×10^{-1} (h^{-1})	Sharova et al. (2009)
μ_{m5}	$3.15 \times 10^{-2} (h^{-1})$	Sharova et al. (2009)
μ_{m6}	1.06×10^{-1} (h^{-1})	Sharova et al. (2009)
μ_{m7}	6.75×10^{-2} (h^{-1})	Sharova et al. (2009)
k_{p1}	80 mol (cell h)$^{-1}$	NCBI NP_001540.2
k_{p2}	316 mol (cell h)$^{-1}$	NCBI NP_003632.3
k_{p3}	298 mol (cell h)$^{-1}$	NCBI AFF60355.1
k_{p4}	90 mol (cell h)$^{-1}$	NCBI NP_150088.1
k_{p5}	110 mol (cell h)$^{-1}$	NCBI AAL50053.1
k_{p6}	125 mol (cell h)$^{-1}$	NCBI NP_066928.1
k_{p7}	61 mol (cell h)$^{-1}$	NCBI AAH90934.1

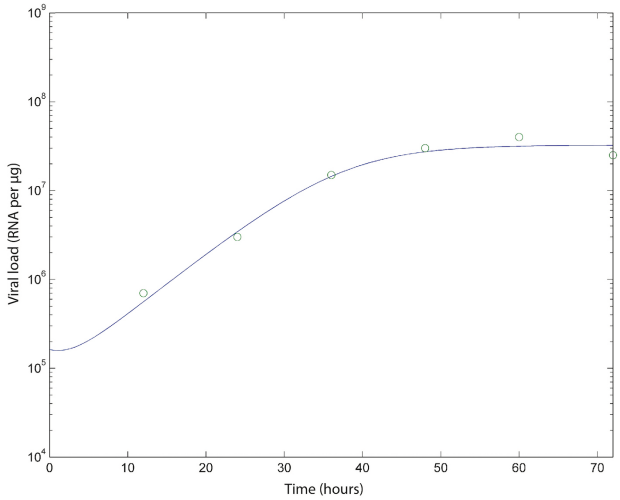

Fig. 2. Model validation against experimental dta. Dynamics of positive strands in infected cells. The green circles correspond to the experimental data and the blue line shows the model prediction. A proportional scale factor of f_s =1.62×10^5 hepatocytes per μg RNA^{-1} was used in order to reproduce the experimental cell concentration.

ered an IFN concentration = 100 UI as the response of the immune systemGaraigorta and Chisari (2009). Simulations described above were repeated. Systematically each feedback loop was eliminated to calculate each line, Fig. 3. The blue line represents the dependence of the stationary states of the ISG proteins on the HCV concentration, and the green line represents the dependence of the HCV concentration on the ISG proteins. The system has three steady states: the first one is a stable state on the lower branch and represents a virus-clearance state(0 molecules/cell), the second one is an unstable state on the middle branch(48 molecules/cell), and the third one is a stable state on the upper branch, and represents a virus persistence state(163 molecules/cell).

New therapeutic approaches have been suggested to treat infectious diseases. For example, during the last years, mRNA-based gene therapy has been investigated to treat infectious diseases prevention, Schlake et al. (2019). Motivated by the above consideration, we investigated whether the transitions between the two branches of stable, steady states become irreversible when ISG proteins are over-expressed on the hepatocyte cell infected with hepatitis C.

First, we analyzed the bifurcation curves. A bifurcation is a set of parameter values where equilibria appear, disappear or change stability. The bifurcation curve maps this change with respect to a bifurcation parameter. We repeated the above simulations by modifying each value of transcription rate k_{m_i} in the range $[0.1, 10]$ times its nominal value. Figure 4A shows bifurcation curves to seven ISG transcription rates, bi-stability without hysteresis is presented. Furthermore, it must be noted that IFITM1 (blue), IFIT3 (red), and IFITM3 (black) are the ISG mRNA curves showing more sensitivity. Bifurcation curves to seven ISG mRNA degradation rates μ_{m_i} are showed in Fig. 4B. Notice that

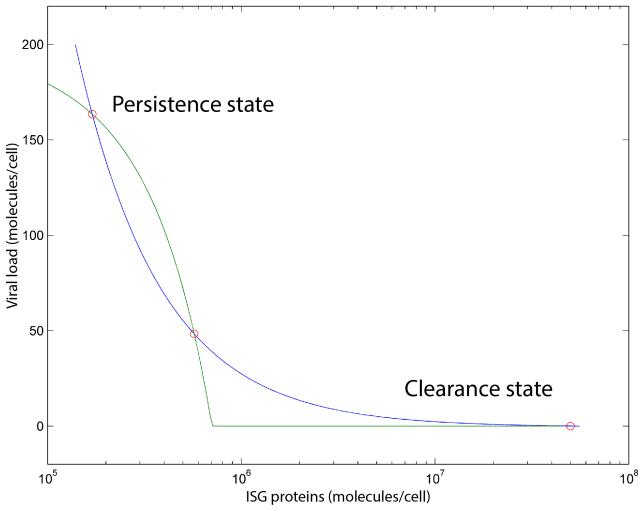

Fig. 3. Steady-state bifurcation curve. Steady states of the viral load as a function of ISG proteins. The model exhibits a bistable switch between clearance (the lowest point) and persistence state (the highest point). The middle point is an unstable threshold.

IFITM1(blue), IFITM3 (black), and IFIT3 (red) are the ISG mRNA degradation curves showing larger sensitivity. Bifurcation curves to translation rates and protein degradation rates are shown in Figs. 4C and 4D, respectively. Clearance state can be achieved with lower parameter changes. We find that IFITM1 transcription rate must be increased at least 80% to obtain the clearance state, IFIT3 transcription rate must be increased at least 300% and IFITM3 transcription rate must be increased at least 500% to obtain the clearance state. We can see that the rest of transcription rates requires an increase in their value above one order magnitude to obtain the clearance state. Similar observations can be noted regarding translational parameters.

Second, recall that mRNA-vaccines based technologies have been investigated extensively for infectious disease prevention and according to the above results, we analyzed a *in-silico* line that produces the over-expression of IFTM1 mRNA. The over-expression is modeled setting the k_{m_1} parameter value in $225 mol(cell h)^{-1}$. Figure 5 shows an irreversible steady state.

We also studied the robustness of bistability on the interaction between HCV and immune response mediated by interferon to global transcription and translation parameter changes. To this end, we fixed the parameters to its nominal value and change the amplification, L. It is the scale parameter to control the global transcription rates. We increased the value of parameter L in the range $[0.8, 1.2]$ by increasing 0.1 units at a time. We performed numeric simulations and computed the corresponding steady states. The obtained results are shown in Fig. 6. We can also appreciate that bistability is present in the global transcription parametric change condition, $L = 0.8$, Fig. 6A. The results of the global parametric-robustness analysis corresponding to the global translation rates are shown in Fig. 6B, $L = 0.1$. Robustness analysis to the rest of

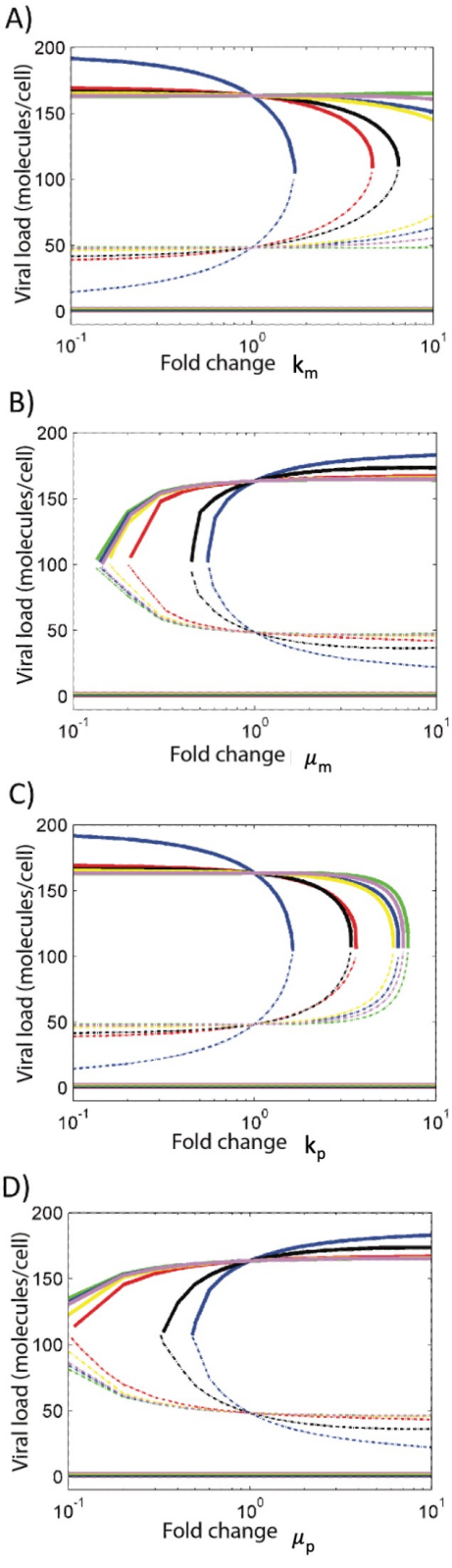

Fig. 4. Bifurcation responses. We started by modifying transcription parameters: A) k_{m_i} B)μ_{m_i}, and translation parameters: C)k_{p_i} D) μ_{p_i}. They were modified in the range [0.1, 10] times its nominal value, one at a time. Color code is IFITM1(blue), IFIT3(red), IFITM3(black), TRIM14(yellow), Viperin(purple), PLSCR1(brown), RNaseL(green). See Eqs. 3 and 4.

amplification values at transcriptional and translational level presented similar results, plots not shown.

4. DISCUSSION

In this work we studied how can the interaction between HCV and immune response mediated by interferon be modulated in infected hepatocyte cells. We did this through a mechanistic model that considers the interaction between the virus and the innate immune response to understand the dynamics of hepatitis C virus. A reduced mathematical model of HCV infection based on the model proposed by Padmanabhan et al. (2014) was presented. Our simulations results reproduce the experimental dynamic viral load reported by Garaigorta and Chisari (2009)(Fig. 2). Bistable responses in the biochemical network of hepatocyte cells infected with HCV in presence of the immune response were found, Fig. 3. These results are in agreement with results reported by Padmanabhan et al. (2014), and they suggest that the deterministic model captures the necessary dynamic characteristics of the system to attempt a further analysis of our hypothesis.

Our results imply that IFITM1 mRNA transcription rate requires the lower change to reach the clearance state than the rest of ISG mRNAs. Similar results are obtained with IFITM1 mRNA degradation rate. Bifurcation plots to translation rates show that IFITM1 translation rate requires the smallest modification to reach the clearance state compared with the rest of ISG proteins. Similar results are obtained with IFITM1 protein degradation rate, Fig. 4. Bistability in virus dynamics has been recently theoretical studied in simian immunodeficiency virus Ciupe et al. (2018). Aguilera and Rodríguez-González (2014) studied bistability in HIV. Our results agrees with Padmanabhan et al. (2014) who shown bistability in HCV.

Bistable cell signaling systems also offer the possibility of providing a sort of biochemical memory, which may contribute to the irreversibility of some cell differentiation processes. Our findings indicate that the cells infected with HCV present bistability. This is consistent with HIV; however, HCV shows bistability without hysteresis. The

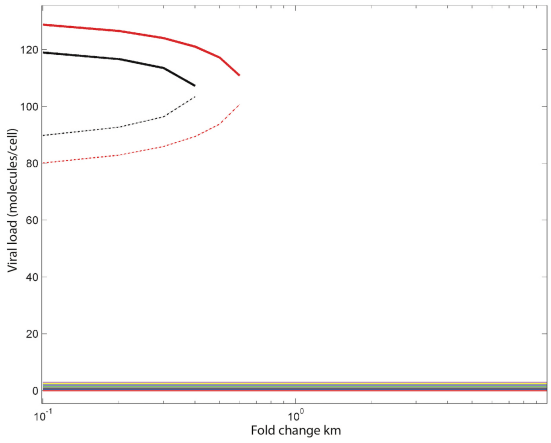

Fig. 5. Effect of over-expressing IFITM1 ISG protein individually. Bifurcation responses to six ISG proteins. The irreversibility of clearance state is shown.

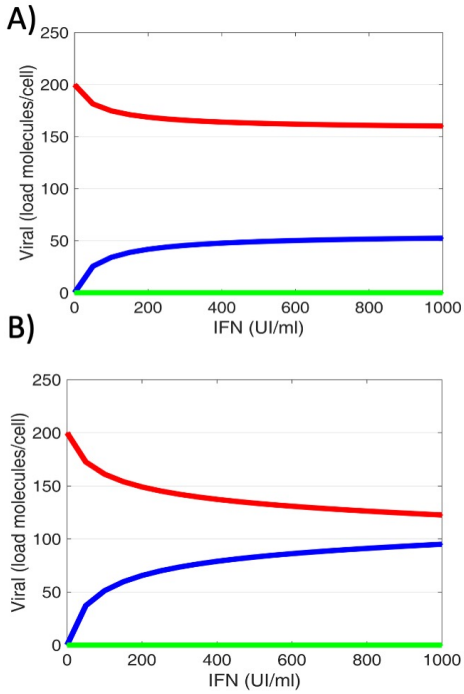

Fig. 6. Comparative plot showing the effect of global transcription and translation parametric changes in bifurcation plot. Bistability is mantained under global changes.

potential significance of hysteresis in biological switching is twofold. A) it decreases the likelihood that a system will repeatedly switch back and forth between two states, a possibility termed chattering when the stimulus that drives the switching is hovering near its threshold value. B) it is a potential mechanism for a type of biochemical memory. As can be seen in Figure 5, the over-expression of IFTM1 mRNA shows irreversible transitions. In an irreversible bistable system, once a system shifts from a low state to a high state, it stays there even when the value of the parameter is set back to a value much lower than that where an earlier shift took place.

Comparing Figs. 4 and 5 shows that it is necessary to decrease transcription rates of IFIT3 (60% its nominal value) or IFITM3(40% its nominal value) to recover bistability, respectively.

Our results indicate that bistability of the interaction between HCV and innate immune response mediated by interferon is robust to global transcription and translation parametric variation.

This study opens several lines of research worth pursuing in future work. It would be worthwhile to extend a similar investigation considering the stochasticity into the viral dynamics in hepatocytes. Furthermore, new experiments in hepatocyte cell lines can be designed.

Finally, our results give insight into hepatitis C virus dynamics in cellular lines and predict how it might be modulated to guarantee the clearance state.

5. CONCLUSION AND FUTURE WORK

We can conclude from these facts that the over-expression of proteins helps to obtain the clearance state in cells infected with HCV in the presence of IFN. In particular, we observed that an intervention strategy involving gene therapy consisting of overexpressing the IFITM1 protein predicts the best efficacy to achieve a virus clearance outcome.

ACKNOWLEDGEMENTS

This work was financially supported by Consejo Nacional de Ciencia y Tecnologa (CONACyT MEXICO) with fellowships to MCA,ARH, and CGL.

REFERENCES

Aguilera, L. and Rodríguez-González, J. (2014). Studying HIV latency by modeling the interaction between HIV proteins and the innate immune response. *Journal of Theoretical Biology*, 360.

Ciupe, S.M., Miller, C.J., and Forde, J.E. (2018). A bistable switch in virus dynamics can explain the differences in disease outcome following SIV infections in rhesus macaques. *Frontiers in Microbiology*, 9, 1–11.

Dennis, P.P. and Bremer, H. (2008). Modulation of Chemical Composition and Other Parameters of the Cell at Different Exponential Growth Rates. *EcoSal Plus*, 3(1). doi:10.1128/ecosal.5.2.3.

Ferrell, J.E. and Xiong, W. (2001). Bistability in cell signaling: How to make continuous processes discontinuous, and reversible processes irreversible. *Chaos*, 11(1), 227–236.

Garaigorta, U. and Chisari, F.V. (2009). Hepatitis C Virus Blocks Interferon Effector Function by Inducing Protein Kinase R Phosphorylation. *Cell Host and Microbe*, 6(6), 513–522.

Guidi, G.M. and Goldbeter, A. (1997). Bistability without hysteresis in chemical reaction systems: A theoretical analysis of irreversible transitions between multiple steady states. *Journal of Physical Chemistry A*, 101(49), 9367–9376.

Metz, P., Reuter, A., Bender, S., and Bartenschlager, R. (2013). Interferon-stimulated genes and their role in controlling hepatitis C virus. *Journal of Hepatology*, 59(6), 1331–1341.

Padmanabhan, P., Garaigorta, U., and Dixit, N.M. (2014). Emergent properties of the interferon-signalling network may underlie the success of hepatitis C treatment. *Nature Communications*, 5, 3872.

Ribeiro, R.M., Li, H., Wang, S., Stoddard, M.B., Learn, G.H., Korber, B.T., Bhattacharya, T., Guedj, J., Parrish, E.H., Hahn, B.H., Shaw, G.M., and Perelson, A.S. (2012). Quantifying the Diversification of Hepatitis C Virus (HCV) during Primary Infection: Estimates of the In Vivo Mutation Rate. *PLoS Pathogens*, 8(8).

Schlake, T., Thess, A., Thran, M., and Jordan, I. (2019). mRNA as novel technology for passive immunotherapy. *Cellular and Molecular Life Sciences*, 76(2), 301–328.

Sharova, L.V., Sharov, A.A., Nedorezov, T., Piao, Y., Shaik, N., and Ko, M.S.H. (2009). Database for mRNA Half-Life of 19 977 Genes Obtained by DNA Microarray Analysis of Pluripotent and Differentiating Mouse Embryonic Stem Cells. *DNA Research*, 16(1), 45–58.

Siwiak, M. and Zielenkiewicz, P. (2013). Transimulation - Protein Biosynthesis Web Service. *PLoS ONE*, 8(9), e73943.